HHS Public Access

Author manuscript

Chembiochem. Author manuscript; available in PMC 2016 July 06.

Published in final edited form as:

Chembiochem. 2015 July 6; 16(10): 1443–1447. doi:10.1002/cbic.201500177.

Salinipyrone and pacificanone are biosynthetic byproducts of the rosamicin polyketide synthase

Takayoshi Awakawa[a,b], **Max Crüsemann**[a], **Jason Munguia**[c], **Nadine Ziemert**[a], **Victor Nizet**[c,d], **William Fenical**[a], and **Bradley S. Moore**[a,d]

Bradley S. Moore: bsmoore@ucsd.edu

[a]Center of Marine Biotechnology and Biomedicine, Scripps Institution of Oceanography, University of California at San Diego, 9500 Gilman Drive, La Jolla, CA 92093-0204 (USA)

[b]Graduate School of Pharmaceutical Sciences, The University of Tokyo, 7-3-1 Hongo, Bunkyo-ku, Tokyo 113-0033 (Japan)

[c]Pediatrics, University of California at San Diego, 9500 Gilman Drive, La Jolla, CA 92093 (USA)

[d]Skaggs School of Pharmacy and Pharmaceutical Sciences, University of California at San Diego, 9500 Gilman Drive, La Jolla, CA 92093 (USA)

Abstract

Salinipyrones and pacificanones are structurally related polyketides from *Salinispora pacifica* CNS-237 proposed to arise from the same modular polyketide synthase (PKS) assembly line. Genome sequencing revealed a large macrolide PKS gene cluster that codes for the biosynthesis of rosamicin A and a series of new macrolide antibiotics. Mutagenesis experiments unexpectedly correlated salinipyrone and pacificanone biosynthesis to the rosamicin octamodule Spr PKS. Remarkably, this bifurcated polyketide pathway illuminates a series of enzymatic domain and module skipping reactions that dictate natural polyketide product diversity. Our findings enlarge the growing knowledge of polyketide biochemistry and illuminate potential challenges in PKS bioengineering.

Keywords

biosynthesis; macrolide antibiotic; polyketide synthase; Salinispora

Salinipyrone A (**1**) and pacificanone A (**2**) are structurally related polyketides produced by the marine bacterium *Salinispora pacifica* CNS-237 (Scheme 1).[1] These natural products share identical lipid tails yet differ in the composition of their lipid head groups, γ-hydroxypyrone versus cyclohexanone, respectively. It has been suggested that the associated polyketide synthase (PKS) may skip the penultimate extension module to yield the slightly smaller salinipyrone product.[1] The concept of module skipping by assembly line, modular PKSs is best illustrated with the methymycin/picromycin system in which 12- and 14-membered ring macrolactones are generated by the same PKS complex adopting alternative

Correspondence to: Bradley S. Moore, bsmoore@ucsd.edu.

Supporting information for this article is given via a link at the end of the document.

conformations to enable an early chain termination in the case of the shorter methymycin aglycone.[2] Module skipping, as well as module stuttering, can lead to biosynthetic diversification in nature as remarkably exemplified with the thalassospiramide family of calpain inhibitors.[3] We thus set out to explore the biosynthetic basis for salinipyrone/pacificanone differentiation and were surprised to learn that while module skipping is indeed a contributing factor, these metabolites are in fact byproducts of an even larger PKS system associated with the rosamicin macrolide antibiotics.

To define the biosynthetic logic of salinipyrone/pacificanone construction, we examined the recently sequenced draft genome of *S. pacifica* CNS-237.[4] Since **2** contains an ethyl side chain in the cyclohexanone unit, we anticipated its biosynthetic origin from the PKS substrate ethylmalonyl-CoA[5] and thus specifically searched for ethylmalonate-specifying acyl transferase (AT) domains within modular PKSs. We identified a single genomic example in a biosynthetic gene cluster fragmented across several contigs. Extensive primer walking completed the DNA sequence of the cluster to give the 23 open reading frame *spr* locus spanning 64.2 kb (GenBank KP997155). This PKS gene cluster shares high sequence homology with that for the macrolide rosamicin A (**3**) (Scheme 1) in *Micromonospora carbonacea* subsp. *aurentiaca* NRRL 2997[6] and contains five PKS genes (*spr7–11*) consisting of eight PKS modules, three cytochrome P450 genes (*spr5–6, -12*),[7] one glycosyltransferase (*spr13*), and genes encoding desosamine biosynthesis (*spr4, 14, 19–20, 22–23*)[8] (Table S1).

Inspection of the chemical structure of the macrolide **3** revealed striking structural similarities to **1** and **2** (Scheme 1), suggesting that all three structure types may originate from the same PKS assembly line. To evaluate this revised biosynthetic hypothesis, we first inactivated the *spr* gene cluster by inserting an apramicin resistance gene cassette (*aac(3)IV*) into the region encoding *spr8–11* by intergenic conjugation (Figure S1). As predicted, the inactivation abolished the production of **1** and a previously unreported derivative, dehydrosalinipyrone A (**4**) (Figure 1A and B), thus confirming that the Spr PKS is responsible for their production (Table S1). Unfortunately, we could not reproduce the production of **2** in the wild-type strain under all fermentation conditions tested, and thus could not positively link its biosynthesis to the *spr* locus. We did, however, observe the loss of five additional compounds in the *spr* mutant never before reported from this bacterium (Figure 1A). Upon isolation and complete spectral analysis,compounds included the known rosamicin analogues **3** and 21-hydroxyrosamicin (izenamicin A3,[9] **5**) along with three novel derivatives, namely 18-dihydro-14-hydroxyrosamicin (**6**), 18-dihydro-21-hydroxyrosamicin (**7**), and 14-hydroxyrosamicin (**8**). We predict that the conserved stereocenters in the new rosamicin analogues **6–8** are identical to those previously reported for **3** and that the new C-14 tertiary hydroxyl stereocenter in **6** and **8** is *S* as in the macrolide mycinamicin II.[10] In the latter case, the cytochrome P450 protein MycG[11] installs the analogous 14*S* hydroxyl group. Of the three cytochrome P450s encoded within the *spr* gene cluster, Spr6 is the most identical with MycG at 45% and is thus a likely candidate for the C-14 hydroxylation. Rosamicins **5–8** exhibit moderate antibacterial properties (Table S10).

The biosynthetic logic of the *spr* gene cluster is consistent with rosamicin octaketides **3, 5–8** in which all eight PKS modules of Spr7–11 are progressively involved in the linear

construction of the macrolide aglycone (Scheme 2A). The smaller salinipyrone hexaketides **1** and **4**, however, are consistent with an incomplete processing by the PKS in which modules 6 and 8 are both skipped. Alternatively, the slightly larger heptaketide **2** could derive by the skipping of just the final PKS module 8. In both cases, the truncated products appear to arise from intermediates independent of the ketoreductase (KR) domain of Spr10 (Scheme 2A), suggesting its role, both directly and indirectly, in product dispersal. To explore this concept, we inactivated the *spr10*-KR domain by introducing a chromosomal point mutation through a single reciprocal recombination event to effectively replace the catalytic tyrosine residue at position 1290 with phenylalanine. Detailed HPLC-MS analyses revealed that the mutant no longer produced the rosamicin octaketides **3, 5–8** but retained **1** and **4**, albeit at lower production titers (Figure 1A). The *spr10*-Y1290F mutant also produced a new product, 18-deoxo-5-deoxy-5-oxotylonolide (**9**), in which the desosamine sugar, the C12-C13 epoxide, and the C18 hydroxyl groups were missing, suggesting that **9** is not a substrate for post-PKS modifying enzymes. We further identified two new compounds with the same molecular composition as **2** and the epimeric pacificanone B (Figure S3), yet due to poor production yields, we were unable to conclusively elucidate their structures.

Inspection of the wild-type *S. pacifica* CNS-237 strain in certain growth media also revealed **9** (Figure S4), albeit at lower levels than the *spr10*-Y1290F mutant strain, suggesting that the Spr10 KR7 domain is naturally partially effective in processing Spr10-linked substrates. We suspect that unreduced β-keto intermediates linked to the module 7-acyl carrier protein (ACP7) also give rise to products in the truncated salinipyrone/pacificanone series, and that their protein offloading may be driven by the innate chemical reactivity of their associated polyketone substrates (Scheme 2B and C). In the case of **1**, this proposal combines a rare intermodule skipping mechanism (module 6) and a domain skipping reaction (KR7) to yield the ACP7-bound salinipyrone intermediate that is likely released through a spontaneous enol lactonization reaction. This biosynthetic bifurcation mediated by module and domain skipping explains the different product outcomes of the Spr PKS in yielding the salinipyrone, pacificanone, and rosamicin natural products, and represents an entirely different mechanism than what we previously reported in the related bacterium *Salinispora arenicola* that co-produces the arenicolide and rifamycin polyketide natural products by off-PKS enzymatic processing.[12] This study further adds to our growing appreciation of the enzymatic complexity of biosynthetic assembly lines[13] and illuminates how much we still need to learn about the structural complexity of these systems to use their full potential in ongoing PKS bioengineering research.

Experimental Section

General

All chemicals were acquired from Fisher Scientific and Sigma–Aldrich and used without further purification. PCR was performed with Takara PrimeStarMax DNA polymerase. Gibson assembly cloning kits were from New England Biolabs. All solvents were of HPLC grade or higher. Analytical HPLC analyses were conducted with an Agilent 1200 HPLC system with diode array detection connected to a Phenomenex Luna C18(2), 250 × 21.5 mm × 10 mm column. LC-MS analyses were conducted with an Agilent 6530 Accurate-Mass Q-

TOF MS (MassHunter software, Agilent) equipped with a Dual electrospray ionization source and an Agilent 1260 LC system (ChemStation software, Agilent) with diode array detector. Preparative HPLC was carried out using an Agilent 218 purification system (ChemStation software, Agilent) equipped with a ProStar 410 automatic injector, an Agilent ProStar UV-Vis Dual Wavelength Detector, and a 440-LC fraction collector connected to Phenomenex Luna C18(2), 10.0 × 250 mm, 5 μm column. NMR data were acquired at the UCSD Skaggs School of Pharmacy and Pharmaceutical Sciences NMR Facility on a 600 MHz Varian NMR spectrometer (Topspin 2.1.6 software, Bruker) with a 1.7 mm cryoprobe.

Construction of *spr* gene inactivation plasmid

A 3.0-kb DNA fragment containing the *spr8*-coding region was amplified by PCR with primer D1f, 5'-**accatgattacgccaagctt**GATTCCCGTCGTTAGCAATGTGACC-3' (overlap sequence boldfaced), and D1r, 5'-**cagctccagcctaca**GACTGGTAGCCGACTGTCGATCTAG-3' (overlap sequence boldfaced), and the chromosome of CNT-237; a 1.1-kb DNA fragment containing *aac(3)IV* and OriT was amplified by PCR with primer AprOriTf, 5'-**AGTCGGCTACCAGTC**TGTAGGCTGGAGCTGCTTC-3' (overlap sequence boldfaced), and AprOriTr, 5'-**GAAACCCATGGCTGACATT**ATTCCGGGGATCCGTCGACC-3' (overlap sequence boldfaced), and pIJ773; and a 3.0-kb DNA fragment containing the Spr11-coding region was amplified by PCR with primer D2f, 5'-**ggtcgacggatccccggaat**AATGTCAGCCATGGGTTTCATTCGG-3' (overlap sequence boldfaced), and D2r, 5'-**aaaacgacggccagtgaattc**CGCGTATTCGGTCATCATCGACAAG-3' (overlap sequence boldfaced), and the chromosome of CNT-237. The three amplified fragments were assembled with a linear pUC19 which is amplified by PCR with primer pUC19f, 5'-gaattcactggccgtcgttttacaac-3', and pUC19r, 5'-aagcttggcgtaatcatggtcatagc-3', resulting in pUC19-Δ*spr*.

Construction of *spr10*-KR point mutation plasmid

A 3.0-kb DNA fragment containing the *Spr10*-coding region was amplified by PCR with primer Spr10KR1f, 5'-**cccccgggctgcaggaattc**CCGGTACGGCGATCAACCAGGAC-3' (overlap sequence boldfaced), and Spr10KR1r, 5'-**GCCCCG*AATG*CTGAT**TGCCCGCCGCTACCCCACACGCCCGCGTTTGAG-3' (overlap sequence boldfaced, the mutated sequence for Y1290F was italicized), and the chromosome of CNT-237; and a 3.0-kb DNA fragment containing the *spr10*-coding region was amplified by PCR with primer Spr10KR2f, 5'-**GGGCAATCAGCA*TTC***GGGGCCGCCAACGCAGCCCTGGACGCAC -3' (overlap sequence boldfaced, the mutated sequence for Y1290F was italicized), and Spr10KR2r, 5'-**ccagcctacacatcgaattc**AGCGGTGCGATCTCTTCCTCGCTG-3' (overlap sequence boldfaced), and the chromosome of CNT-237. The two amplified fragments were assembled with a linear pIJ773 which is amplified by PCR with primer pIJ773f, 5'-gaattcctgcagcccgggggatc-3', and pIJ773r, 5'-gaattcgatgtgtaggctggag-3', resulting in pIJ773-*spr10*.

Introducing plasmids into *S. pacifica* CNT-237 for the inactivation of *spr* and the point mutation of the Spr10KR

pUC19-Δ*spr* and pIJ773-*spr10* were separately introduced into *E. coli* S17-1 cells by electroporation and then transferred into *S. pacifica* CNS-237 by intergeneric conjugation. Mutants, in which the apramycin resistance cassette was integrated into the *S. pacifica* chromosome, were selected on A1 agar by overlaying plates with 200 μgmL^{-1} apramycin and 100 μgmL^{-1} nalidixic acid. Following incubation at 28°C for 7–9 days, exconjugants were randomly selected and those exhibiting an Apr^{r} (for pUC19-Δ*spr*) or Apr^{s} phenotype (for pIJ773-*spr10*) were evaluated by PCR and DNA sequencing for double crossover mutation, respectively. Primer set-1 (f, 5'-AGACCGCTGTGGAAGAACAGATCG-3' and r, 5'-gaacttcgaagcagctccagcctac-3') and primer set-2 (f, 5'-cttattcgcacctggcggtgctcaacg-3' and r, 5'-CGCTAACGGGGGATGTCATAATCTGC-3') were used for the PCR for the evaluation of Δ*spr* strain. 595-bp fragment amplified by KRpcrf, 5'-gaacttcgaagcagctccagcctac-3' and KRpcrr, 5'-CGCGGTGAACAGATCCCAATCCACGTC-3' was sequenced for the evaluation of *spr10-Y1290F* strain.

Comparative metabolite profiling between wild type and mutant *S. pacifica* strains

Wild type *S. pacifica* CNS-237 and the mutants prepared above were grown in 1.0 L liquid seawater-based A1+BFe medium (10 g starch, 4 g yeast extract, 2 g, peptone, 1 g $CaCO_3$, 40 mg $Fe_2(SO_4)_3$•$4H_2O$, 100 mg KBr) for 11 days at 28°C with shaking at 230 rpm. 20 mL of the whole culture was extracted by EtOAc, and the resulting extract was concentrated to dryness *in vacuo* and dissolved with 500 μL CH_3OH. HPLC analyses were conducted with a flow rate of 1.5 mLmin^{-1} and a gradient from 10–100% CH_3CN (0.1% TFA)/water (0.1% TFA) for 90 min, and LC-MS analyses were conducted with a flow rate of 0.7 mLmin^{-1} and mobile phase gradient from 10–100% CH_3CN (0.1% formic acid)/water (0.1% formic acid) for 23 min with positive mode ESI.

Preparation of 5–8

S. pacifica CNS-237 was cultured in five 2.8 L Fernbach flasks, each containing 1.0 L of seawater-based A1-BFe medium and shaken at 230 rpm at 27°C. After seven days of cultivation, HP-20 resin was added to adsorb the organic products, and the culture and resin were stirred for 1.5 h. The resin was filtered by a glass column, washed with deionized water, and eluted with CH_3OH. The methanol was removed under reduced pressure, and the resulting aqueous layer was extracted with 100:5 CH_2Cl_2:CH_3OH. The extract was subjected to silica-gel column chromatography using a CH_2Cl_2:CH_3OH stepwise gradient system (100:5, 100:7.5, 100:10 and 100:20). The fraction containing **7–8** (100:10) was purified by reversed-phase preparative HPLC using a gradient of 10–55% CH_3CN (0.1% TFA)/water (0.1% TFA) for 30 min twice to afford 0.3 mg of **8**, and 0.2 mg of **7**. The fraction containing **5–6** (100:20) was purified by reversed-phase preparative HPLC using a gradient of 10–50% CH_3CN (0.1% TFA)/water (0.1% TFA) for 30 min to afford 0.5 mg of **6**, and 0.1 mg of **5**.

Preparation of 3

S. pacifica CNS-237 was cultured in three 2.8 L Fernbach flasks, containing 1.0 L of seawater-based A1-BFe medium and shaken at 230 rpm at 27°C. After seven days of cultivation, the whole culture was extracted by EtOAc, and the resulting extract was concentrated to dryness *in vacuo*. The extract was subjected to silica-gel column chromatography using a CH_2Cl_2:CH_3OH stepwise gradient system (100:0, 100:1, 100:2, 100:3, 100:4 and 100:5). The fraction containing **3** (100:2) was purified by reversed-phase preparative HPLC using a gradient of 10–60% CH_3CN (0.1% TFA)/water (0.1% TFA) for 40 min to afford 0.5 mg of **3**.

Preparation of 1 and 4

S. pacifica CNS-237 was cultured in a 2.8 L Fernbach flask, containing 1.0 L of seawater-based A1-BFe medium and shaken at 230 rpm at 27°C for 3 days. 25 mL of the culture was transferred into another 2.8 L Fernbach flask, containing 1.0 L of seawater-based A1-BFe medium and shaken at 200 rpm at 27°C. After seven days of cultivation, the whole culture was extracted with EtOAc, and the resulting extract was concentrated to dryness *in vacuo*. The extract was subjected to silica-gel column chromatography using a CH_2Cl_2:CH_3OH stepwise gradient system (100:0, 100:1, 100:3, 100:4 and 100:5). The fractions containing **1** (100:4 and 100:5) were purified by reversed-phase preparative HPLC using 45% CH_3CN (0.1% TFA)/water (0.1% TFA) for 40 min to afford 0.4 mg of **1**. The fractions containing **4** (100:3) were purified by reversed-phase preparative HPLC using 50% CH_3CN (0.1% TFA)/water (0.1% TFA) for 40 min to afford 0.3 mg of **4**.

Preparation of 9

The *spr10Y1290F* strain was cultured in four 2.8 L Fernbach flasks, each containing 1.0 L of seawater-based A1-production medium (10 g starch, 4 g yeast extract, 2 g, peptone, 1 g $CaCO_3$) and shaken at 230 rpm at 27°C. After seven days of cultivation, the whole culture was extracted with EtOAc, and the resulting extract was concentrated to dryness *in vacuo*. The extract was subjected to silica-gel column chromatography using a CH_2Cl_2:CH_3OH stepwise gradient system (100:0, 100:1, 100:3 and 100:5). The fraction containing **9** (100:3) was purified by reversed-phase preparative HPLC using 40% CH_3CN (0.1% TFA)/water (0.1% TFA) for 40 min to afford 0.8 mg of **9**.

Spectroscopic data

Salinipyrone A (1): yellow oil; $[\alpha]_D^{25.9}$ = −76.2 (*c* = 0.33, CH_3OH); ^1H- and ^{13}C-NMR: see Table S2; HR-ESI-MS (positive) *m/z* 293.1760 $[M+H]^+$ (calcd for $C_{17}H_{25}O_4$ 293.1747).

Rosamicin A (3): white powder; $[\alpha]_D^{26.6}$ = −25.4 (*c* = 0.30, EtOH); ^1H- and ^{13}C-NMR: see Table S7; HR-ESI-MS (positive) *m/z* 582.3660 $[M+H]^+$ (calcd for $C_{31}H_{52}NO_9$ 582.3636).

Dehydrosalinipyrone A (4): yellow oil; $[\alpha]_D^{26.3}$ = +30.6 (*c* = 0.33, CH_3OH); ^1H- and ^{13}C-NMR: see Table S8; HR-ESI-MS (positive) *m/z* 291.1605 $[M+H]^+$ (calcd for $C_{17}H_{23}O_4$ 291.1590).

18-Dihydro-21-hydroxyrosamicin (5): white powder; $[\alpha]_D^{27.4} = -18.8$ (*c* = 0.30, EtOH); ^{1}H- and ^{13}C-NMR: see Table S4; HR-ESI-MS (positive) *m/z* 600.3751 $[M+H]^+$ (calcd for $C_{31}H_{54}NO_{10}$ 600.3742).

18-Dihydro-14-hydroxyrosamicin (6): white powder; $[\alpha]_D^{27.4} = -27.8$ (*c* = 0.30, EtOH); ^{1}H- and ^{13}C-NMR: see Table S3; HR-ESI-MS (positive) *m/z* 600.3768 $[M+H]^+$ (calcd for $C_{31}H_{54}NO_{10}$ 600.3742).

21-Hydroxyrosamicin (izenamicin A3) (7): white powder; $[\alpha]_D^{27.4} = -34.9$ (*c* = 0.30, EtOH); ^{1}H- and ^{13}C-NMR: see Table S6; HR-ESI-MS (positive) *m/z* 598.3580 $[M+H]^+$ (calcd for $C_{31}H_{52}NO_{10}$ 598.3586).

14-Hydroxyrosamicin (8): white powder; $[\alpha]_D^{27.4} = -2.4$ (*c* = 0.30, EtOH); ^{1}H- and ^{13}C-NMR: see Table S5; HR-ESI-MS (positive) *m/z* 598.3584 $[M+H]^+$ (calcd for $C_{31}H_{52}NO_{10}$ 598.3586).

18-Deoxo-5-deoxy-5-oxotylonolide (9): white powder; $[\alpha]_D^{27.4} = +33.6$ (*c* = 0.30, EtOH); ^{1}H- and ^{13}C-NMR: see Table S9; HR-ESI-MS (positive) *m/z* 431.2426 $[M+Na]^+$ (calcd for $C_{23}H_{36}O_6Na$ 431.2410).

Supplementary Material

Refer to Web version on PubMed Central for supplementary material.

Acknowledgements

We thank our UCSD colleagues B. M. Duggan for assistance with NMR data acquisition and analysis, P.R. Jensen for materials and helpful advise, and E. O'Neill, S. Diethelm, K. Murata, and C.A. Kauffman for discussions. Funding was generously provided by NIH grant GM085770 to B.S.M. and the Uehara Memorial Foundation via a postdoctoral fellowship to T.A.

References

1. a) Oh D, Gontang EA, Kauffman CA, Jensen PR, Fenical W. J. Nat. Prod. 2008; 71:570–575. [PubMed: 18321059] b) Jensen PR, Moore BS, Fenical W. Nat. Prod. Rep. 2015
2. a) Xue Y, Sherman DH. Nature. 2000; 403:571–575. [PubMed: 10676969] b) Beck BJ, Yoon YJ, Reynolds KA, Sherman DH. Chem. Biol. 2002; 9:575–583. [PubMed: 12031664] c) Kittendorf JD, Beck BJ, Buchholz TJ, Seufert W, Sherman DH. Chem. Biol. 2007; 14:944–954. [PubMed: 17719493] d) Kittendorf JD, Sherman DH. Bioorg. Med. Chem. 2009; 17:2137–2146. [PubMed: 19027305]
3. Ross A, Xu Y, Lu L, Kersten RD, Shao Z, Al-Suwailem AM, Dorrestein PC, Qian P, Moore BS. J. Am. Chem. Soc. 2013; 135:1155–1162. [PubMed: 23270364]
4. Ziemert N, Lechner A, Wietz M, Millán-Aguiñaga N, Chavarria KL, Jensen PR. Proc. Natl. Acad. Sci. U. S. A. 2014; 111:E1130–E1139. [PubMed: 24616526]
5. Wilson MC, Moore BS. Nat. Prod. Rep. 2012; 29:72–86. [PubMed: 22124767]
6. Farnet, CM.; Staffa, A.; Yang, X. United States Patent US. 20030113874. 2002.
7. Iizaka Y, Higashi N, Ishida M, Oiwa R, Ichikawa Y, Takeda M, Anzai Y, Kato F. Antimicrob. Agents Chemother. 2013; 57:1529–1531. [PubMed: 23274670]
8. Zhao L, Sherman DH, Liu H. J. Am. Chem. Soc. 1998; 120:10256–10257.
9. Imai H, Suzuki K, Morioka M, Sakaki T, Tanaka K, Kadota S, Iwanami M, Saito T, Eiki H. J. Antibiot. 1989; 42:1000–1002. [PubMed: 2737942]

10. a) Hayashi M, Kinoshita K, Satoi S, Nakatsu K. J. Antibiot. 1982; 35:1243–1244. [PubMed: 7142027] b) Kinoshita K, Satoi S, Hayashi M, Harada K, Suzuki M, Nakatsu K. J. Antibiot. 1985; 38:522–526. [PubMed: 4008346] c) Kinoshita K, Satoi S, Hayashi M, Nakatsu K. J. Antibiot. 1989; 42:1003–1005. [PubMed: 2737943]
11. a) Anzai Y, Li S, Chaulagain MR, Kinoshita K, Kato F, Montgomery J, Sherman DH. Chem. Biol. 2008; 15:950–959. [PubMed: 18804032] b) Li S, Tietz DR, Rutaganira FU, Kells PM, Anzai Y, Kato F, Pochapsky TC, Sherman DH, Podust LM. J. Biol. Chem. 2012; 287:37880–37890. [PubMed: 22952225]
12. Wilson MC, Gulder TAM, Mahmud T, Moore BS. J. Am. Chem. Soc. 2010; 132:12757–12765. [PubMed: 20726561]
13. Khosla C, Herschlag D, Cane DE, Walsh CT. Biochemistry. 2014; 53:2875–2883. [PubMed: 24779441]

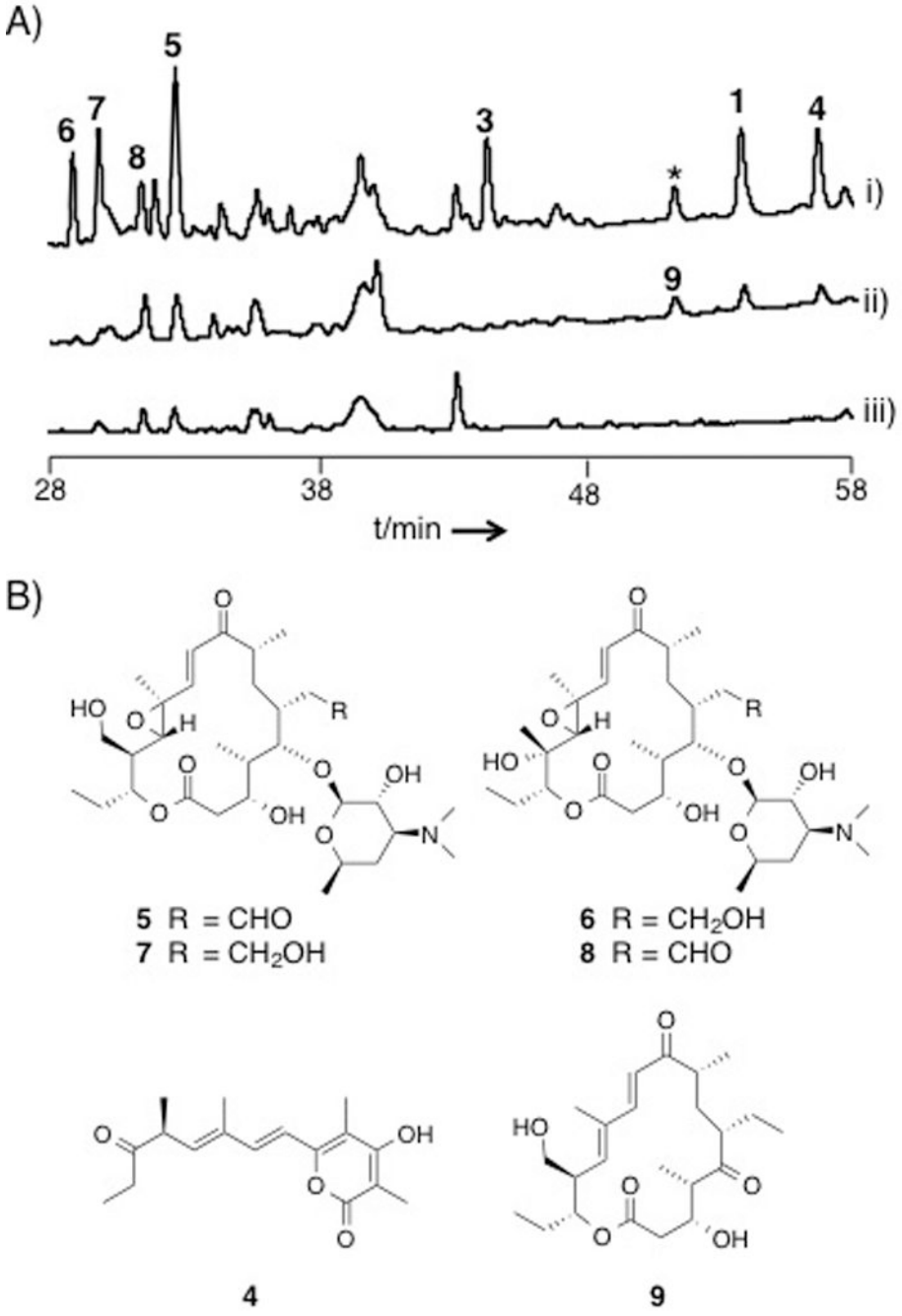

Figure 1.

(A) HPLC chromatograms of the metabolites from i) CNS-237 wild-type, ii) *spr10*Y1290F, and iii) Δ*spr* cultured in A1FeBC medium. The traces represent chromatograms acquired by detection at 254 nm. (* indicates the compound whose MS and UV spectrum are identical to **1**.) Though **9** is eluted at the same RT as the compound marked with an asterisk, the peak of **9** is detected at 280 nm only in the Y1290F strain (Figure S2). (B) Chemical structures of **4**–**9**.

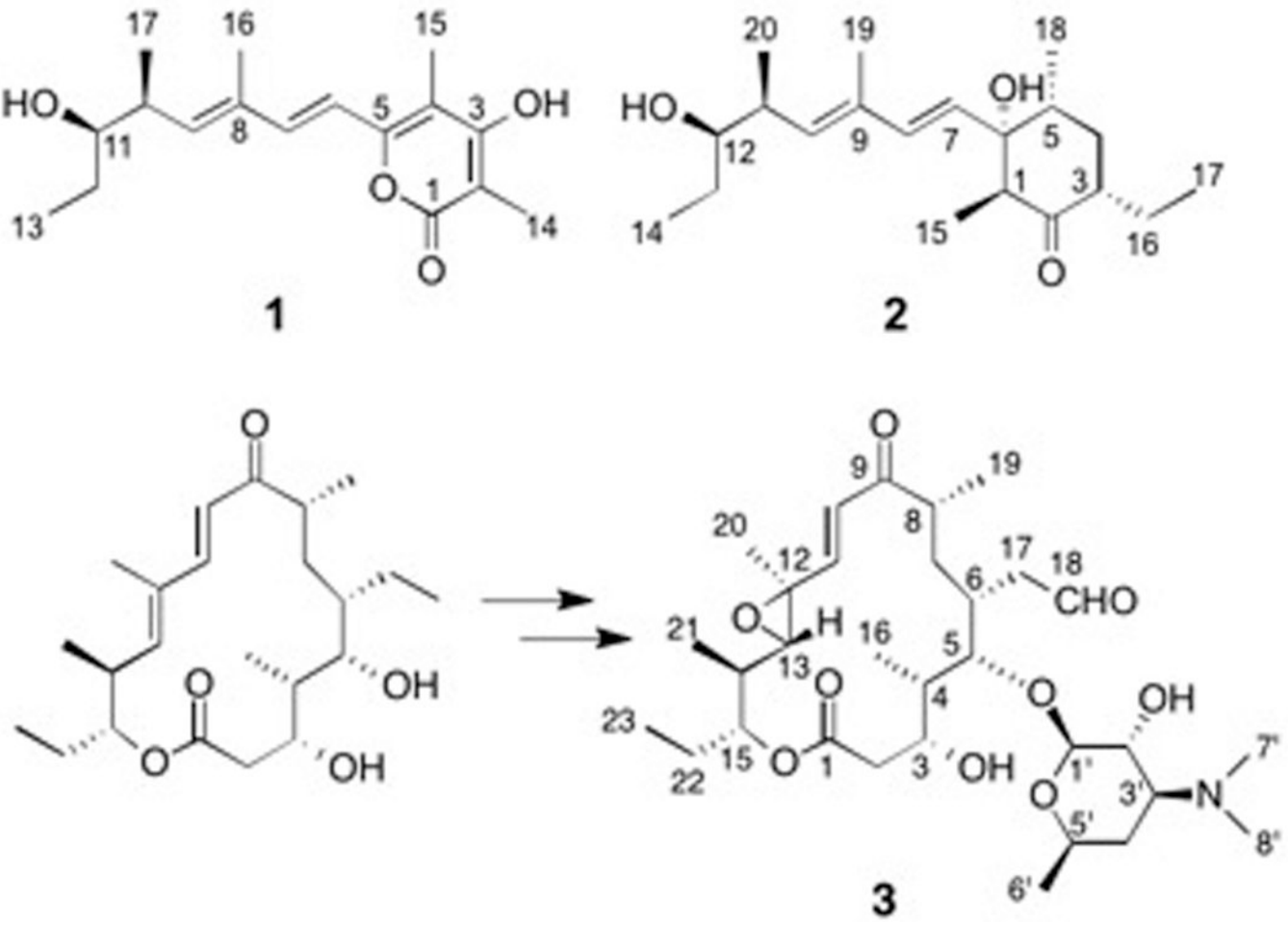

Scheme 1.
The chemical structures of salinipyrone A (**1**), pacificanone A (**2**), and rosamicin A (**3**)

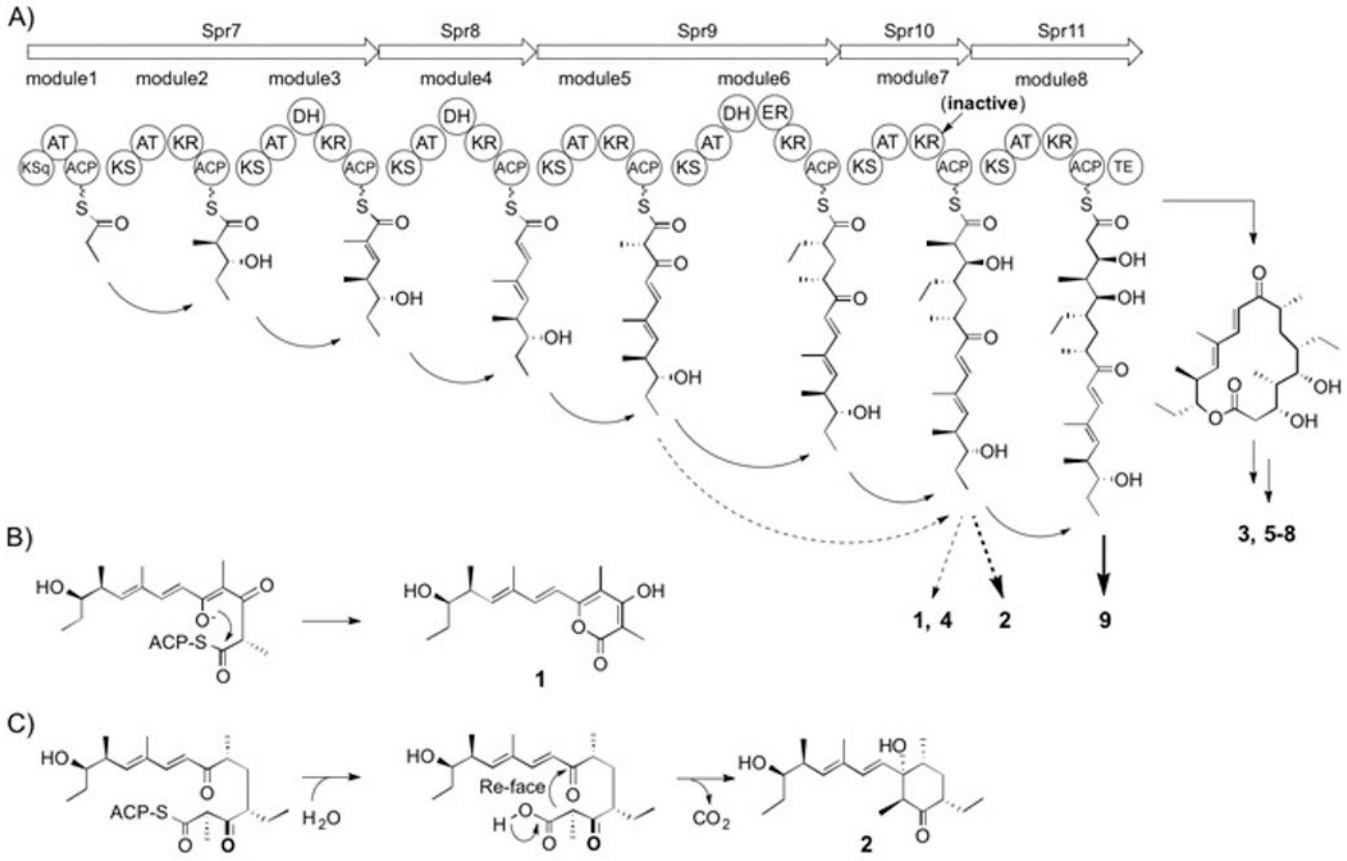

Scheme 2.

Proposed biosynthesis of **1–9**. (A) Spr PKS organization and deduced assembly of **1–9**. The arrows depict the sequential synthesis of intermediates leading to the mature products **3** and **5–8**. The dotted arrows represent module skipping movements leading to **1** and **4**. The bold arrow shows the assembly of **9**, while the bold dotted arrow leading to **2** involves the skipping of the final module. In both cases, the KR domain in module 7 is inactive. The formation of **1** (B) and **2** (C) involve reactions on premature ACP-bound intermediates.